

KINETICS OF COLLISION PROCESSES IN DILUTE NOBLE GASES

René KALUS

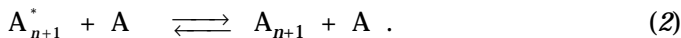
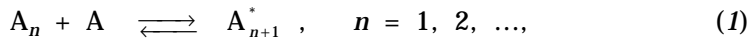
Department of Physics, University of Ostrava, Bráfova 7, 701 03 Ostrava 1, Czech Republic;
e-mail: rene.kalus@osu.cz

Received August 13, 1999
Accepted November 22, 1999

Kinetics of collision processes is analyzed for dilute noble gases within a linear approximation. Dilute gas is treated as a chemically reacting mixture of dimers and monomers. Two elementary reaction models are analyzed employing theoretical rate constants calculated recently from quasiclassical trajectories. Stability of stationary states and relaxation of small concentration perturbations are treated in terms of linearized kinetic equations. The results obtained are generalized for heavier noble gases (neon to xenon). Helium is, because of quantum nature, analyzed separately.

Key words: Gas-phase chemistry; Reaction mechanisms; Kinetics; Noble gases; Argon; Clusters; van der Waals interactions.

Collisions involving small van der Waals clusters play an important role during the initial stage of homogeneous nucleation in non-perfect gases. In particular, the very beginning of the nucleation process, when subcritical clusters (up to 15–20 particles) are formed, is completely governed by the kinetics of recombination and dissociation processes¹



In reactions (1) and (2), asterisks denote energetically unstable clusters, which decay rapidly due to excess of internal energy, unless they are stabilized in a subsequent collision. On the other hand, as a consequence of weakness of van der Waals bonds, energetically stable clusters are frequently dissociated in collisions, even at low temperatures. Since the monomer concentration exceeds by orders of magnitude that of all the other aggregates present in dilute gas, only collisions of clusters with

monomers are taken into account. Cluster-cluster collisions are usually ignored.

Reaction chain (1)–(2) starts with formation of the simplest, two-particle clusters – dimers. Thus, detailed knowledge of processes involving dimers is of principal importance since they are immediate precursors of all the other sub- and supercritical clusters. An important role that dimers play in the initial stage of homogeneous nucleation has been well known for a long time, so they have been studied both experimentally² and theoretically³. Noble gases, in particular argon, are usually employed as a prototype nucleating system. The main reason for this is that the interaction forces are known with high accuracy for noble gases, which is of crucial importance in theoretical studies.

According to reactions (1) and (2), dimers are formed by a two-step mechanism. First, an unstable dimer appears in a binary monomer collision

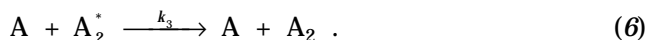
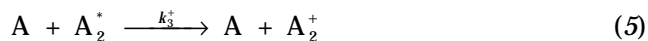


The unstable dimer is a collision complex, usually defined by a proximity criterion: if the distance between the colliding monomers is below some maximum value, r_{\max} , the collision aggregate is called unstable dimer; otherwise, the particles are considered free. The maximum distance, r_{\max} , corresponds to the interaction radius and must be chosen large enough. If so, measurable results of the theory are r_{\max} -independent⁴. Unstable dimers decay spontaneously

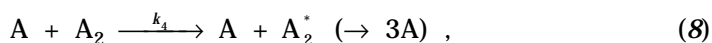
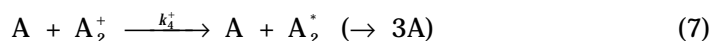


if they are not affected by a third body. Second, unstable dimer may be stabilized in a collision with a third body, preferably a monomer. In such stabilization collisions, two types of dimers are formed: stable dimer and metastable dimer. The former has a negative internal energy, representing a bound two-particle system. The latter is rotationally excited and bears a positive internal energy, which is, however, below the centrifugal barrier of the effective potential energy curve (see Fig. 1). Although the metastable dimers are classically bound, they can decay spontaneously by the quantum mechanical tunneling. Significance of noble gas metastables was recognized long before^{5,6} and they must be taken into account for a model of

collision processes in dilute noble gases to be realistic. Let A_2 and A_2^+ denote stable and metastable dimers, respectively, then the stabilization reactions may be written as follows⁷



In addition to the stabilization processes, collision-induced dissociation of stabilized dimers⁷



and transitions between stables and metastables,

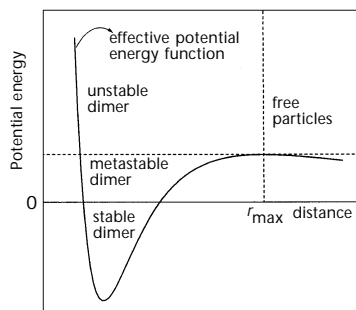
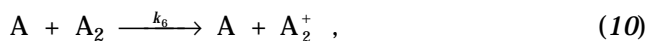


FIG. 1
A typical effective noble gas potential energy curve for a small value of rotation quantum number

take place in dilute noble gases. Both processes must be considered, even at low temperatures, because of extremely shallow minima in noble gas two-body interaction potentials.

As mentioned above, metastable dimers decay spontaneously by a quantum mechanical tunneling through the centrifugal barrier



The reverse process is also possible



Although they may be important, these processes are ignored in this study because the rate coefficients for reactions (11) and (12) are not known at present, except for results of a preliminary calculation performed recently using the WKB (Wentzel–Kramers–Brillouin) approximation⁸. To fill this gap, we are performing accurate quantum mechanical calculations of quasistationary states in noble gas dimers now.

Cluster–cluster collisions are usually ignored in literature because of their negligible probability in a dilute gas. Nevertheless, some previous studies seem to indicate that the cluster–cluster collisions may be important, *e.g.* for the formation of stabilized argon trimers⁹. To our knowledge, rate constants for dimer–dimer collision processes are not available at present, however. Thus, these processes are not considered in this study.

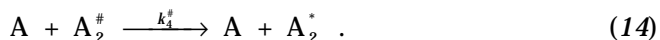
Below, recently calculated^{8,10,11} values of the rate coefficients for reactions (3)–(10) are employed in an analysis of stationary states as well as relaxation processes in dilute noble gases. Two models of elementary collision processes are formulated and analyzed separately so that importance of the transitions between stables and metastables, not previously assumed in literature, can be assessed. The conditions for thermal equilibrium in chemically reacting mixtures are employed in a calculation of stationary concentrations of noble gas dimers and monomers. Relaxation of small perturbations of the equilibrium concentrations is analyzed in terms of linearized kinetic equations.

THEORETICAL

Collision Processes in Dilute Gases

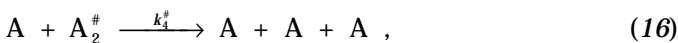
With accuracy up to the second order of magnitude of the overall particle density, non-perfect dilute gas can be described¹⁰ as a mixture of monomers and dimers participating in reactions (3)–(12). This approximate picture may be fairly realistic for the very beginning of homogeneous nucleation, when monomers and dimers are the only significant clusters and the larger van der Waals complexes may be ignored. Provided the rate coefficients for reactions (3)–(12) are available, a thorough analysis of the initial stage of homogeneous nucleation can be performed. Recently, theoretical values of rate coefficients were calculated for reactions (3)–(10) for all the noble gases using quasiclassical trajectory methods^{11,12}. They are surveyed in the following paragraph. In this paper, we employ them in kinetic analysis. Two models of elementary processes in dilute noble gases are analyzed below:

Standard model. This model is usually considered in literature. Stable and metastable dimers are not distinguished, processes (9)–(12) are not included. Let $A_2^{\#}$ denote a stabilized (stable or metastable) dimer, then the standard model is given by the following processes



Rapid equilibrium is often assumed⁷ for reactions (3) and (4), which reduces the above scheme to a couple of processes – ternary recombination and collision-induced dissociation:





where $k_r^{\#} = (k_1/k_2)k_3^{\#}$

Extended model. Within this model, stable and metastable dimers are distinguished explicitly; however, both formation and decay of metastables *via* quantum tunneling through the rotational barrier are ignored. Thus, reactions (3)–(10) are involved in the extended model.

Reaction Rate Coefficients

Recently, rate coefficients for reactions (3)–(10) were calculated^{11,12} using quasiclassical trajectory (QCT) methods¹³. The QCT methods consist in numerical integration of classical equations of motion for the collision trajectories, the initial conditions of which are chosen properly. Batches of classical trajectories are then averaged to get the desired macroscopic reaction parameters, such as the reaction cross sections and the rate coefficients. In the above calculations, the initial conditions were generated to simulate a thermally equilibrium gas. Classical statistics was used for translation degrees of freedom of colliding systems, both classical and quasiclassical statistics were used for rotations and vibrations of noble gas dimers. Except helium, the classical and quasiclassical rate coefficients correspond to each other with high accuracy¹². Thus, the classical approximation seems to be valid for the heavier noble gases (neon, xenon). On the other hand, classical approach completely fails for helium. Therefore, quasiclassical data are employed for helium in the following.

Accuracy of QCT data crucially depends on the potential energy surfaces used. In the above calculations, the potential energy surface was constructed as a sum of pairwise contributions using sophisticated pair functions by Aziz and collaborators – HFDID1 for argon¹⁴ and HFDB-2 for the other noble gases¹⁵. According to the data published previously¹⁶, many-body contributions to the interaction energy were ignored.

All the rate coefficients are temperature-dependent, some of them depending on the interaction radius, r_{\max} . These dependences can be represented by simple analytical formulae. For example, the following expressions can be obtained¹¹ for the rate coefficients k_1 and k_2

$$k_1^{\#} = 2\pi^{1/2} r_{\max}^{* - 2} \sqrt{T^*} \quad (17)$$

$$k_2^* = \frac{1.7028 \pm 0.0014}{r_{\max}^*} \sqrt{T^*}, \quad (18)$$

where reduced, dimensionless quantities are used: $r_{\max}^* = r_{\max} / r_m$, $T^* = k_B T / \varepsilon$, $k_1^* = k_1 / [r_m^2 \sqrt{\varepsilon / m}]$ and $k_2^* = k_2 / [(1/r_m) \sqrt{\varepsilon / m}]$. Here, ε and r_m stand for the depth and the position of the minimum in the pair potential, respectively, m being mass of a noble gas atom, and k_B is the Boltzmann constant.

The recombination rate constants, $k_r^+ = (k_1/k_2)k_3^+$ and $k_r = (k_1/k_2)k_3$, for the ternary processes



are r_{\max} -independent¹¹. Their temperature dependence can be represented by a simple, Arrhenius-like formula¹¹

$$k_r = AT^{C_1} \exp(C_2 T), \quad (21)$$

which corresponds to a quadratic temperature dependence of the activation energy, $E_{\text{act}} = E_{\text{act}}^0 + C_1 T + C_2 T^2$, with $E_{\text{act}}^0 = 0$. Suppose dimensionless quantities $T^* = k_B T / \varepsilon$ and $k_r^* = k_r / r_m^5 \sqrt{\varepsilon / m}$ are used; then, for the heavier noble gases (neon to xenon), the temperature dependence of recombination rate constants, k_r^+ and k_r , can be represented by universal functions, $k_r^{+*}(T^*)$ and $k_r^*(T^*)$, respectively, which allows the results to be generalized for all the noble gases, except helium¹¹. Necessary adjustable parameters, which were obtained from least-squares fits to the QCT data, are summarized in Table I.

Similarly, the rate constants for the dissociation processes, reactions (7) and (8), and those for the transitions between stables and metastables, reactions (9) and (10), are r_{\max} -independent. Temperature dependence of dissociation and stable to metastable transition rate constants can be represented by¹²

TABLE I

Numerical values of the adjustable parameters used in analytical representation of ternary noble gas atom-atom recombination rate coefficients, $3 A \xrightarrow{k_r^+} A + A_2^+$, $3 A \xrightarrow{k_r} A + A_2$

Rate coefficient	<i>A</i>	<i>C</i> ₁	<i>C</i> ₂
<i>k</i> _r ⁺	20.45 ± 0.64	-0.155 ± 0.019	-0.421 ± 0.024
<i>k</i> _r	19.76 ± 0.39	-0.278 ± 0.010	-0.445 ± 0.016

TABLE II

Numerical values of the adjustable parameters used in analytical representation of dissociation rate coefficients, $A + A_2^+ \xrightarrow{k_4^+} 3 A$, $A + A_2 \xrightarrow{k_4} 3 A$

Rate coefficient	<i>A</i>	<i>E</i> _{act} ⁰	<i>C</i> ₁
<i>k</i> ₄ ⁺	14.33 ± 0.23	0.151 ± 0.014	0.424 ± 0.011
<i>k</i> ₄	10.44 ± 0.22	0.561 ± 0.021	0.419 ± 0.013
<i>k</i> ₄ (He)	53.57 ± 0.03	0.0	0.368 ± 0.001

TABLE III

Numerical values of the adjustable parameters used in analytical representations of rate coefficients for transitions between stable and metastable dimers, $A + A_2^+ \xrightarrow{k_5} A + A_2$, $A + A_2 \xrightarrow{k_6} A + A_2^+$

Rate coefficient	<i>A</i>	<i>E</i> _{act} ⁰	<i>C</i> ₁	<i>C</i> ₂
<i>k</i> ₅	6.505 ± 0.056	0.0	-0.0712 ± 0.0095	0.0377 ± 0.0066
<i>k</i> ₆	5.487 ± 0.074	0.443 ± 0.012	0.0582 ± 0.0094	0.0

$$k = AT^{C_1} \exp\left(-\frac{E_{\text{act}}^0}{k_B T}\right), \quad (22)$$

which corresponds to a linear temperature dependence of the activation energy, $E_{\text{act}} = E_{\text{act}}^0 + C_1 T$, whereas Eq. (21) is applicable¹² to the metastable-to-stable transition. Again, reduced quantities T^* and $k_n^* = k_n / r_m^2 \sqrt{\epsilon / m}$, $n = 4, 5$, and 6 , are used, which allows the results to be generalized for all the noble gases, except helium¹². Numerical values of the adjustable parameters are summarized in Tables II and III. As no metastable states exist for weakly bound helium dimer¹⁷, no data are shown for the processes involving helium metastables in Tables I-III.

RESULTS AND DISCUSSIONS

Thermal Equilibrium in Monomer-Dimer Mixture

The equilibrium concentrations of noble gas monomers and dimers can be found, within the above kinetic models, as a stationary solution of the corresponding kinetic equations. Alternatively, they can be determined using the conditions of thermodynamic equilibrium in a chemically reacting mixture¹⁸. Clearly, if the kinetic models are correct, thermodynamic results must correspond to those obtained from kinetic considerations, and *vice versa*. A more detailed analysis of the problem is given elsewhere¹⁰. The following may be observed from this analysis: (i) if only monomers and dimers are taken into account and the higher-order clusters are ignored, the equilibrium concentrations obtained from kinetics are accurate up to the second order of magnitude of the overall particle density, c ; and (ii) the stationary concentrations obtained from kinetics correspond to those obtained using statistical thermodynamics, at least up to the second order of magnitude of the overall particle density, as long as the rate coefficients for the reactions involved obey some constraints. In our QCT calculations, those constraints were used to verify reliability of the computational data¹¹.

Let c_{10} , c_{20}^* , c_{20}^+ , and c_{20} represent the equilibrium concentrations of monomers, unstable dimers, metastable dimers, and stable dimers, respectively. Then, the following expressions can be obtained from statistical thermodynamics

$$c_{10} = c - 2\zeta z_2^{(\text{int})} c^2 \pm \dots \quad (23)$$

$$c_{20}^* = \zeta z_2^* c^2 \pm \dots \quad (24)$$

$$c_{20}^+ = \zeta z_2^+ c^2 \pm \dots \quad (25)$$

$$c_{20} = \zeta z_2 c^2 \pm \dots \quad (26)$$

Here, z_2^* , z_2^+ , and z_2 denote internal partition functions for unstable, metastable, and stable dimers, respectively, $z_2^{(\text{int})} = z_2^* + z_2^+ + z_2$, and $\xi = [h^2 / (\pi m k_B T)]^{3/2}$, where h is the Planck constant. Reduced, dimensionless concentrations, $c^* = c r_m^3$, are used throughout this study. As an illustration of Eqs (23)–(26), the equilibrium concentrations of argon dimers are shown in Fig. 2 over a range of reduced temperatures $T^* = 0.3\text{--}3.5$ (40–500 K for argon). In this figure, $c^* = 0.00141$ (which corresponds to the pressure of 10^5 Pa at 0 °C for argon), and $r_{\text{max}}^* = 2.53$ ($9.5 \cdot 10^{-10}$ m for argon). The theoretical value of the amount of stabilized dimers obtained for 0 °C, about 1%, corresponds rather well to the experimental results².

Relaxation in Dilute Gases

Relaxation of small monomer and dimer concentration perturbations towards the equilibrium is analyzed below. The standard model and the extended model are treated separately.

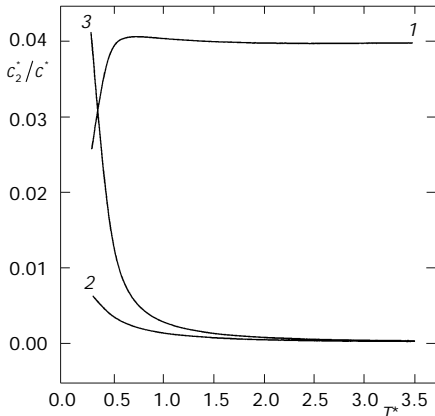


FIG. 2
Relative concentrations of stable, metastable, and unstable dimers in dilute argon ($c^* = 0.00141$, $r_{\text{max}}^* = 2.53$): 1 unstable, 2 metastable, and 3 stable

Standard model. Within the standard model, the time evolutions of the monomer and dimer concentrations are governed by the following kinetic equations:

$$\frac{dc_1}{dt} = -2k_1 c_1^2 + 2k_2 c_2^* \quad (27)$$

$$\frac{dc_2^*}{dt} = k_1 c_1^2 - k_2 c_2^* - k_3^* c_1 c_2^* + k_4^* c_1 c_2^* \quad (28)$$

$$\frac{dc_2^*}{dt} = k_3^* c_1 c_2^* - k_4^* c_1 c_2^* , \quad (29)$$

where the standard model rate coefficients k_3^* and k_4^* are given as follows:

$$k_3^* = k_3^+ + k_3 \quad (30)$$

$$k_4^* = \frac{Z_2^+}{Z_2^+ + Z_2} k_4^+ + \frac{Z_2}{Z_2^+ + Z_2} k_4^- . \quad (31)$$

In Eq. (31), equilibrium occupation of both stable and metastable rotation-vibration states is assumed. In other words, rapid equilibrium is assumed for the transitions between stables and metastables, $A_2 + A \rightleftharpoons A_2^+ + A$. If the volume of the system and the number of atoms are kept constant, the particle conservation law,

$$c_1 + 2(c_2^* + c_2^*) = c , \quad (32)$$

must be obeyed. Here, $c_2^* \equiv c_2^+ + c_2^-$ denotes the concentration of stabilized (both stable and metastable) dimers.

Stationary concentrations, c_{10} , c_{20}^* , and c_{20}^* , can be obtained by solving Eqs (27)–(29) with the left-hand sides set zero. As mentioned above, the stationary concentrations correspond, at least up to the second order of magnitude of the overall particle density, c , to the equilibrium concentrations given by Eqs (23)–(26). If the stationary concentrations are perturbed by small perturbations, $c'_1 = c_1 - c_{10}$, $c'^*_2 = c^*_2 - c^*_{20}$, and $c'^*_{20} = c^*_{20} - c^*_{20}$, they will

relax back to the equilibrium in accordance with the following linearized kinetic equations:

$$\frac{dc_1'}{dt} = -4k_1 c_{10} c_1' + 2k_2 c_2^* \quad (33)$$

$$\frac{dc_2^*'}{dt} = (2k_1 c_{10} - k_3^* c_{20}^* + k_4^* c_{20}^*) c_1' - (k_2 + k_3^* c_{10}) c_2^* + k_4^* c_{10} c_2^* \quad (34)$$

$$\frac{dc_2^*'}{dt} = (k_3^* c_{20}^* - k_4^* c_{20}^*) c_1' + k_3^* c_{10} c_2^* - k_4^* c_{10} c_2^* \quad (35)$$

Clearly, the particle conservation law must be obeyed,

$$c_1' + 2(c_2^* + c_2^*) = 0 \quad (36)$$

Equations (33)–(35) can be solved, after c_1' has been excluded using Eq. (36), in a standard way,

$$\begin{pmatrix} c_2^* \\ c_2^* \end{pmatrix}' = A \begin{pmatrix} x_1 \\ y_1 \end{pmatrix} \exp(-t/\tau_1) + B \begin{pmatrix} x_2 \\ y_2 \end{pmatrix} \exp(-t/\tau_2) \quad (37)$$

The relaxation times, τ_1 and τ_2 , are then given as follows:

$$\frac{1}{\tau_1} = k_2 + (4k_1 + k_3^*)c - \frac{k_3^*}{k_2}(4k_1 - k_4^*)c^2 \pm \dots \quad (38)$$

$$\frac{1}{\tau_2} = k_4^* c - \frac{k_1}{k_2} \left(2k_4^* - 2k_3^* + \frac{k_3^* k_4^*}{k_1} \right) c^2 \pm \dots \quad (39)$$

In the following, dimensionless relaxation times, $\tau^* = \tau / (r_m \sqrt{m/\varepsilon})$, are used.

If rapid equilibrium is assumed for $A + A \rightleftharpoons A_2^*$, kinetic equations (27)–(29) simplify to

$$\frac{dc_2^*}{dt} = k_r^* c_1^3 - k_4^* c_1 c_2^* \quad (40)$$

and the particle conservation law (32) transforms to

$$c_1 + 2 \left(\frac{k_1}{k_2} c_1^2 + c_2^{\#} \right) = c, \quad (41)$$

where $k_r^{\#} \equiv (k_1/k_2)k_3^{\#}$. Clearly, stationary solution of Eqs (40) and (41) is identical to that of Eqs (27)–(29), and (32); relaxation towards equilibrium is different, however. Linearized equations (40) and (41) yield $c_2^{\#} = A \exp(-t/\tau)$, where

$$\frac{1}{\tau} = k_4^{\#} c - 2 \frac{k_1}{k_2} (k_4^{\#} - k_3^{\#}) c^2 \pm \dots \quad (42)$$

It is clear from Eq. (42) that the relaxation time τ corresponds to the relaxation time τ_2 of the standard model, Eq. (39). The relaxation time τ_1 is equal zero now, because it corresponds to the relaxation processes pertinent to the violation of equilibrium for $A + A \rightleftharpoons A_2^*$, which is not admitted in the present case.

Curves representing temperature dependence of the relaxation times τ_1 , τ_2 , and τ are shown in Fig. 3. Since the relaxation times depend, more or less, on the interaction radius, r_{\max} , and the overall particle density, c , several curves, obtained for different values of r_{\max} and c , are displayed in Fig. 3. The following may be observed in this figure:

(a) Within the standard model, two relaxation modes exist, the characteristic times of which, τ_1 and τ_2 , are different by orders of magnitude. It is clear from Eqs (38) and (39) that τ_1 corresponds predominantly to the rapid processes of formation and spontaneous decay of unstable dimers, reactions (3) and (4), whilst much slower stabilization and dissociation processes, reactions (5)–(8), affect primarily τ_2 .

(b) The longer relaxation time, τ_2 , depends strongly on the overall particle density, c , whereas the shorter one, τ_1 , is almost c -independent.

(c) Dependence on the interaction radius, r_{\max} , is much more apparent for the shorter relaxation time. This is also clear from Eq. (38): the zero-order expansion term of the right-hand side of Eq. (38) is r_{\max} -dependent, whereas the same dependence does not appear for τ_2 before the second-order term; see Eq. (39).

(d) Both τ_1 and τ_2 are positive. Thus, the stationary state of the standard model is asymptotically stable.

(e) If equilibrium in $A + A \rightleftharpoons A_2^*$ is assumed, a relaxation time is obtained that is rather close to the standard model longer characteristic time, τ_2 . This means that the assumption of rapid equilibrium is rather plausible for the formation and the decay of unstable dimers, $A + A \rightleftharpoons A_2^*$.

Extended model. For this model, within which stable and metastable dimers are distinguished explicitly, the kinetic equations read as follows:

$$\frac{dc_1}{dt} = -2k_1 c_1^2 + 2k_2 c_2^* \quad (43)$$

$$\frac{dc_2^*}{dt} = k_1 c_1^2 - k_2 c_2^* - (k_3^+ + k_3) c_1 c_2^* + k_4^+ c_1 c_2^* + k_4 c_1 c_2 \quad (44)$$

$$\frac{dc_2^+}{dt} = k_3^+ c_1 c_2^* - (k_4^+ + k_5) c_1 c_2^* + k_6 c_1 c_2 \quad (45)$$

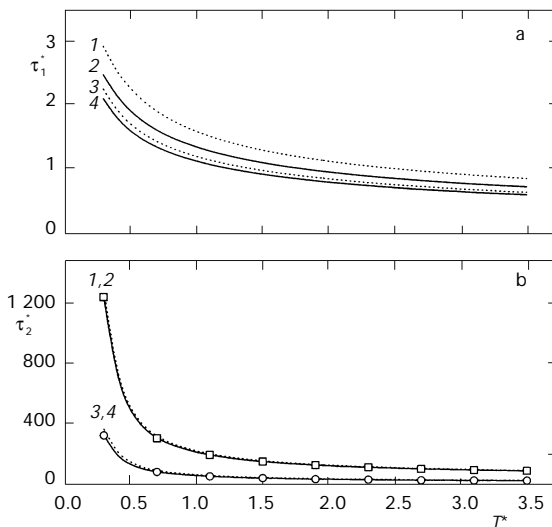


FIG. 3
Characteristic relaxation times for the standard reaction model as a function of temperature; a rapid relaxation mode, b slow relaxation mode (□, ○ results obtained if rapid equilibrium for $A + A \rightleftharpoons A_2^*$ is assumed): 1 $c^* = 0.00064$, $r_{\max}^* = 3.2$ ($12.0 \cdot 10^{-10}$ m for argon), 2 $c^* = 0.00064$, $r_{\max}^* = 2.53$ ($9.5 \cdot 10^{-10}$ m), 3 $c^* = 0.00256$, $r_{\max}^* = 3.2$ ($12.0 \cdot 10^{-10}$ m), 4 $c^* = 0.00256$, $r_{\max}^* = 2.53$ ($9.5 \cdot 10^{-10}$ m)

$$\frac{dc_2}{dt} = k_3 c_1 c_2^* + k_5 c_1 c_2^+ - (k_4 + k_6) c_1 c_2 \quad (46)$$

and the particle conservation law gains the following form

$$c_1 + 2(c_2^* + c_2^+ + c_2) = c. \quad (47)$$

Again, the time evolution of small concentration perturbations is described within the linear approximation. After the atom conservation condition for the concentration perturbations, $c'_1 + 2(c_2^{*'} + c_2^{+'} + c_2') = 0$, is employed to exclude the monomer concentration, c'_1 , Eqs (43)–(46) can be written in a form of three linear ordinary differential equations for three unknown, time-dependent functions, $c_2^{*'}, c_2^{+'}$, and c_2' . Solution of these equations can be found in a standard way, which yields three characteristic times. To avoid unnecessary complexity, overall particle density expansions up to the first order of magnitude are given below:

$$\frac{1}{\tau_1} = k_2 + (4k_1 + k_3^+ + k_3) c \pm \dots \quad (48)$$

$$\frac{1}{\tau_2} = \left\{ \frac{k_4 + k_4^+ + k_5 + k_6}{2} \left[1 + \sqrt{1 - \frac{k_4^+ k_4 + k_4^+ k_6 + k_4 k_5}{(k_4 + k_4^+ + k_5 + k_6)^2}} \right] \right\} c \pm \dots \quad (49)$$

$$\frac{1}{\tau_2} = \left\{ \frac{k_4 + k_4^+ + k_5 + k_6}{2} \left[1 - \sqrt{1 - \frac{k_4^+ k_4 + k_4^+ k_6 + k_4 k_5}{(k_4 + k_4^+ + k_5 + k_6)^2}} \right] \right\} c \pm \dots \quad (50)$$

Temperature dependence curves for the relaxation times given by Eqs (48)–(50), as well as those of the standard model, are shown in Fig. 4. The following conclusions can be made from this figure:

(a) The extended model characteristic times are positive for the temperatures assumed, at least up to the first order of magnitude with respect to the overall particle density. Thus, the stationary solution of Eqs (43)–(47) is asymptotically stable.

(b) The relaxation times differ significantly from each other. The fastest process relaxation time, τ_1 , is still much smaller than both τ_2 and $\tilde{\tau}_2$. Therefore, the assumption of rapid equilibrium is well acceptable for $A + A \rightleftharpoons A_2^*$, even within the extended model. On the other hand, the difference be-

tween the longest time, τ_2 , and the medium one, $\tilde{\tau}_2$, is much smaller than the difference between τ_2 and τ_1 . This means that for the transitions $A + A_2 \rightleftharpoons A + A_2^+$ the assumption of rapid equilibrium, adopted within the standard model, may be of a limited validity.

(c) There is an evident correspondence between the relaxation times τ_1 and τ_2 obtained from the present model and those from the standard model. The deviations are only about several per cent for all the temperatures considered. As mentioned above, τ_1 and τ_2 correspond mainly to the formation and spontaneous decay of unstable dimers, and to the stabilization and dissociation processes, respectively. The new relaxation time, $\tilde{\tau}_2$,

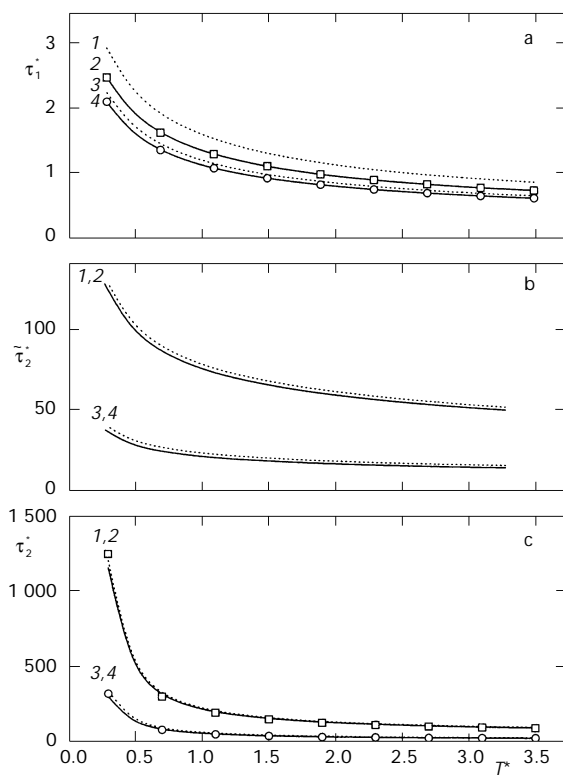


FIG. 4

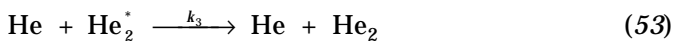
Characteristic relaxation times for the extended reaction model as a function of temperature; a-c relaxation modes (\square , \circ results obtained from the standard model): 1 $c^* = 0.00064$, $r_{\max}^* = 3.2$ ($12.0 \cdot 10^{-10}$ m for argon), 2 $c^* = 0.00064$, $r_{\max}^* = 2.53$ ($9.5 \cdot 10^{-10}$ m), 3 $c^* = 0.00256$, $r_{\max}^* = 3.2$ ($12.0 \cdot 10^{-10}$ m), 4 $c^* = 0.00256$, $r_{\max}^* = 2.53$ ($9.5 \cdot 10^{-10}$ m)

seems to correspond primarily to the transitions between stables and metastables, reactions (9) and (10).

(d) The longer relaxation times, τ_2 and $\tilde{\tau}_2$, depend significantly on the overall particle density, c , whilst the same dependence is much less apparent for τ_1 . On the other hand, both longer characteristic times do not significantly depend on the interaction radius, r_{\max} . They are even r_{\max} -independent within the linear approximation with respect to c . The dependence of τ_1 on r_{\max} is, however, well pronounced.

Helium. As mentioned above, the classical data, on which the generalized formulae used for the heavier noble gases are based, are not correct for helium, since they differ significantly from the corresponding quasiclassical data. In this paragraph, quasiclassical rate constants^{8,12} are used to perform a similar analysis for helium such as that presented above for the heavier noble gases. Clearly, we are aware of limits of the quasiclassical approach, which may not be fully adequate for light helium atoms.

If the quasiclassical rate constants are employed, instead of the classical ones, the following is taken into account: (i) helium dimer has only one bound state, the dissociation energy of which is very small¹⁷ (about $1.6 \cdot 10^{-3}$ K), and (ii) no metastable, quasibound state exists in helium dimer¹⁷. Thus, no reactions involving helium metastables occur in a realistic reaction model:



In Eqs (51)–(54), asterisk denotes, in accordance with the convention used throughout this study, an unstable dimer. Evidently, reactions (51)–(54) are the same as those of the standard model, provided the following substitutions are made: $k_3 \rightarrow k_3^*$, $k_4 \rightarrow k_4^*$, and $c_2 \rightarrow c_2^*$. Thus, the kinetic equations corresponding to reactions (51)–(54) can be analyzed in the exactly same

way as those of the standard model. The characteristic relaxation times, obtained from such an analysis, are summarized in Fig. 5. It is clear from this figure that the shorter relaxation time is not much affected by the quantum effects mentioned above. However, this can be expected, since the dominant, zero-order term on the right-hand side of Eq. (38) is of purely classical nature within the present approach. On the other hand, remarkable differences are apparent between the classical characteristic time and the quasiclassical one for the slow relaxation mode, τ_2 ; cf. Figs 3 and 5. For lower temperatures, reduced values of the quasiclassical time obtained for helium are 10–20 times smaller than the corresponding classical ones. Even for higher temperatures, this difference is still well apparent, although less dramatic (4–6 times).

CONCLUSIONS

Theoretical reaction rate constants, obtained recently from quasiclassical trajectory calculations^{11,12}, have been employed in an analysis of the thermal equilibrium and the relaxation processes in dilute noble gases. A model

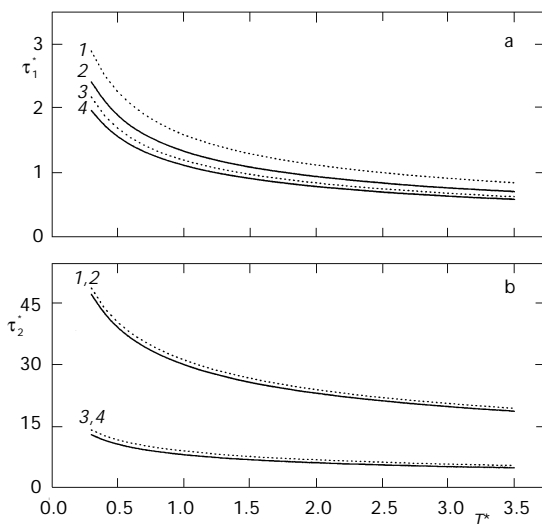


FIG. 5

Characteristic relaxation times for helium as a function of temperature; a rapid relaxation mode, b slow relaxation mode: 1 $c^* = 0.00064$, $r_{\max}^* = 3.2$ ($9.5 \cdot 10^{-10}$ m for helium), 2 $c^* = 0.00064$, $r_{\max}^* = 2.53$ ($7.4 \cdot 10^{-10}$ m), 3 $c^* = 0.00256$, $r_{\max}^* = 3.2$ ($9.5 \cdot 10^{-10}$ m), 4 $c^* = 0.00256$, $r_{\max}^* = 2.53$ ($7.4 \cdot 10^{-10}$ m)

of a chemically reacting mixture of monomers and dimers has been used to describe a dilute gas, which, as shown elsewhere, yields results accurate up to the second order of magnitude with respect to the overall particle density¹⁰. Two models of elementary reaction processes have been formulated and analyzed within the linear stability theory. For heavier noble gases (neon to xenon), classical rate constants have been used and the results have been presented in a generalized form. Some quantum effects have been taken into account for helium and the results obtained within the quasiclassical approximation have been presented separately.

Both metastable and unstable dimers play an important role in dilute noble gases. For the former, this conclusion is in accordance with other studies⁵. On the other hand, unstable dimers are not usually taken into account in literature. According to the results obtained, ignoring them may lead to serious errors, *e.g.* in calculation of the second virial coefficient⁸. Thus, all three types of noble gas dimers – stable, metastable, and unstable – have been taken into account in the present study.

Relaxation of slightly perturbed monomer and dimer equilibrium concentrations has been studied using linearized kinetic equations; characteristic relaxation times have been obtained for both models of elementary reaction processes. In particular, two relaxation modes have been detected, the characteristic times of which, τ_1 and τ_2 , differ significantly, by orders of magnitude at lower temperatures. For example, for argon we get $\tau_1 \approx 5 \cdot 10^{-12}$ s and $\tau_2 \approx 10^{-9}$ s at the nitrogen boiling temperature (77.3 K) and for the overall particle concentration $c^* = 0.00064$. This value of c^* corresponds to a pressure of 50 kPa at 0 °C for argon. It follows from the above analysis that the rapid relaxation mode is predominantly influenced by the formation and spontaneous decay of unstable dimers, *i.e.* by very rapid atom-atom collisions. On the other hand, the slow relaxation mode corresponds to the stabilization and dissociation processes induced by collisions of dimers with monomers, *i.e.* to infrequent three-atom collisions. The rapid equilibrium for processes $A + A \rightleftharpoons A_2^*$, often assumed in literature, is shown to be rather plausible for the temperatures involved.

Most of the QCT rate coefficients used in this work were calculated on the computers belonging to the Supercomputing Centre of Charles University, Prague, and the Supercomputing Centre of the Institute of Mining and Metallurgy, Ostrava. The work was in part supported by the grant No. 3708/96 of University of Ostrava, and the grant No. 13/98 of Faculty of Science, University of Ostrava.

REFERENCES

1. a) Pal P., Hoare M. R.: *J. Phys. Chem.* **1987**, *91*, 2474; b) Wegener P. P.: *J. Phys. Chem.* **1987**, *91*, 2479.
2. a) Milne T. A., Vandegrift E., Green F. T.: *J. Chem. Phys.* **1970**, *52*, 1552; b) Worsnop D. R., Buelow S. J., Herschbach D. R.: *J. Phys. Chem.* **1986**, *90*, 5121.
3. a) Schieve W. C., Harrison H. W.: *J. Chem. Phys.* **1974**, *61*, 700; b) DelleDonne M., Howard R. E., Roberts R. E.: *J. Chem. Phys.* **1976**, *64*, 3387; c) Howard R. E., Roberts R. E., DelleDonne M.: *J. Chem. Phys.* **1976**, *65*, 3067; d) Thompson D. L., Raff L. M.: *J. Chem. Phys.* **1982**, *76*, 301; e) Thompson D. L.: *J. Chem. Phys.* **1982**, *76*, 1806; f) Turner R. A., Raff L. M., Thompson D. L.: *J. Chem. Phys.* **1984**, *80*, 3189; g) Hahn S. J., Kim S. K.: *J. Phys. Chem.* **1993**, *97*, 2072.
4. Hill T. L.: *J. Chem. Phys.* **1955**, *23*, 617.
5. Stogryn D. E., Hirschfelder J. O.: *J. Chem. Phys.* **1959**, *31*, 1531.
6. a) Thompson D. L., Raff L. M.: *J. Chem. Phys.* **1982**, *76*, 301; b) Turner R. A., Raff L. M., Thompson D. L.: *J. Chem. Phys.* **1984**, *80*, 3189.
7. Howard R. E., Planck T. L., Trussell S. R., Saadevandi B.: *Chem. Phys. Lett.* **1987**, *142*, 33.
8. Kalus R.: *Ph.D. Thesis*. Prague Institute of Chemical Technology, Prague 1998
9. Thompson D. L.: *J. Chem. Phys.* **1982**, *77*, 1269.
10. Kalus R.: *Acta Fac. Rerum Nat. Univ. Ostraviensis, Phys.-Chem.* **1997**, *157*, 7.
11. Kalus R.: *J. Chem. Phys.* **1998**, *109*, 8289.
12. Kalus R.: *J. Chem. Phys.* **1999**, *110*, 3856.
13. Karplus M., Porter R. N., Sharma R. D.: *J. Chem. Phys.* **1965**, *43*, 3259.
14. Aziz R. A.: *J. Chem. Phys.* **1993**, *99*, 4518.
15. a) Aziz R. A., Janzen A. R.: *Phys. Rev. Lett.* **1995**, *74*, 1586; b) Aziz R. A., Meath W. J., Allnatt A. R.: *Chem. Phys.* **1983**, *78*, 295; c) Aziz R. A., Slaman M. J.: *Mol. Phys.* **1986**, *58*, 679; d) Aziz R. A., Slaman M. J.: *Mol. Phys.* **1986**, *57*, 825.
16. Howard R. E., Roberts R. E., DelleDonne M.: *J. Chem. Phys.* **1976**, *65*, 3067.
17. Aziz R. A., Janzen A. R.: *Phys. Rev. Lett.* **1995**, *74*, 1586.
18. Samohýl I.: *Racionální termodynamika chemicky reagujících směsí*, 1st ed., p. 248. Academia, Praha 1982.